JET–P(97)07

Transfer Rates of Toroidal Angular Momentum during Neutral Beam Injection

K-D Zastrow, W G F Core, L-G Eriksson,
M G von Hellermann, A C Howman, R W T König.

JET Joint Undertaking, Abingdon, Oxfordshire, OX14 3EA, UK.

Preprint of a paper to be submitted for publication in
Nuclear Fusion

April 1997

ABSTRACT

At the onset of neutral beam injection in JET the toroidal angular momentum is observed to rise instantaneously in the outer regions of the plasma. The toroidal angular momentum in the plasma centre, where the fast ions are injected into passing orbits, and the thermal energy are found to rise on the slowing down time scale of the fast ions. This behaviour can be explained by a model that incorporates three mechanisms for momentum transfer of fast ions to the bulk: 1) Instantaneous, or first orbit, transfer which results from particles that are injected into trapped orbits, 2) Collisional transfer of momentum from passing ions during their slowing down process, 3) Finally, once the particles have thermalised they enhance the total angular momentum of the rotating plasma.

The model for the torque is applied to the study of toroidal angular momentum confinement in transient hot-ion H-mode plasmas in JET. In contrast to steady-state conditions, like L-Mode and ELMy H-Mode where the toroidal angular momentum confinement time τ_L is approximately equal to the thermal energy confinement time τ_E, τ_L is found to be about a factor of two smaller than τ_E in the ELM-free phase of the discharge. This can be explained by the reduction of conductive and convective transport losses in this phase, so that charge exchange with recycling and gas puff neutrals, which is always present, gains importance. Ions carry approximately half of the energy in the edge, whereas they carry all the momentum. Since only the ions are affected by charge-exchange we observe a reduction of τ_L relative to τ_E by up to factor of two.

1. INTRODUCTION

Confinement times of thermal energy and toroidal angular momentum with neutral beam injection (NBI) co-parallel to the plasma current are about equal under steady state conditions [0]. However for studies under transient plasma conditions it is not sufficient to equate the rate of toroidal angular momentum transfer from the neutral beams to the reservoir of fast ions with the torque exerted on the bulk plasma by the fast ions. It is important to model the different mechanisms of momentum transfer, in order to take the time scale on which the transfer occurs into account. If all fast ion momentum was transferred during the slowing down process, we would find the total torque and the total power to have comparable overall time behaviour. Hence, as long as the confinement times are similar, we would expect comparable behaviour for the rate of rise of energy and momentum at the onset of NBI. In this paper we present experimental evidence that this is not the case, and that momentum is transferred faster than energy. This, to our knowledge, is the first time that this difference has been demonstrated.

To account for this observation we describe the torque on the bulk plasma by instantaneous torque and collisional torque. The latter is calculated using an analytical solution to the Fokker-

Planck equation [1]. The instantaneous torque is due to radial movements of fast ions during their first orbit and the corresponding displacement currents of the background and is obtained from considerations of momentum conservation [2]. In a different approach, Monte Carlo models have been developed to calculate the radial profiles of momentum transfer [3,4]. In the following we discuss the two methods.

Within the framework of the Monte-Carlo model there are three contributions to the total torque: $\vec{j} \times \vec{B}$ forces which arise from any radial movement of the fast ions, collisional slowing down and thermalisation. The particles are followed during their slowing down until they have reached a specified energy. They are then counted as thermal, and the remaining momentum is added to the bulk plasma.

In the analytical model it is convenient to carry out the integration over the velocity of the ions between the injection velocity and v=0, i.e. until they have come to rest in the rotating plasma frame. In the laboratory frame there is an additional term similar in concept to the thermalisation torque mentioned above: when particles are added to the bulk they also enhance the toroidal angular momentum. We will call this contribution the transformation torque.

The comparison is more complicated for the $\vec{j} \times \vec{B}$ term. In the Monte-Carlo model this torque is accounted for in each calculation step for each particle by keeping the canonical angular momentum constant between collisions. However, since the fast ions lose and gain momentum due to $\vec{j} \times \vec{B}$ forces, a large number of particles have to be followed to obtain sufficient accuracy. Otherwise the calculated results are very noisy and hence not well suited to the study of angular momentum confinement in transient plasma conditions.

In the analytical model treatment used here we evaluate the difference in toroidal angular momentum between the first orbit average and the injected toroidal momentum and then apply the slowing down calculation to the first orbit average. For particles injected into passing orbits on the outboard side the average will be smaller than the injected toroidal angular momentum, and for particles injected on the inboard side it will be larger. Since there are more particles absorbed on the outboard side this results in a small instantaneous net torque on the bulk. For particles injected into trapped orbits, however, there is a large instantaneous torque since here the first orbit average momentum is small.

The outline of the paper is as follows. In section 2 we show the time evolution of toroidal angular momentum and thermal energy at the onset of NBI which clearly demonstrates that angular momentum is transferred faster than energy from the beams, and that this enhanced transfer occurs in the outer regions of the plasma, rather than in the plasma centre. In section 3 we discuss the momentum transfer mechanisms in more detail. Finally in section 4 we apply the model to the calculation of the toroidal angular momentum confinement time in transient hot-ion H-mode plasmas.

2. BEHAVIOUR OF TOROIDAL ANGULAR MOMENTUM

2.1. Experimental procedure

We obtain the total angular momentum of thermal particles and, for comparison, the thermal energy by integration of local measurements over the corresponding flux volume elements. The radial profile of the electron density n_e is obtained from LIDAR, cross-calibrated using the time evolution as obtained from interferometry. The electron temperature T_e is obtained from ECE, whilst the radial profiles of helium, beryllium and carbon density, ion temperature T_i and frequency of toroidal rotation ω are measured with visible charge exchange spectroscopy. Ion temperature and rotation frequency are corrected for cross-section effects [5,6]. All data are mapped on a flux surface grid calculated with the equilibrium code EFIT [7].

The toroidal angular momentum density on thermal particles of a flux surface is given by local measurements as

$$\mathrm{I} = \sum_i m_i n_i \omega \Theta \equiv \langle m \rangle n_e \omega \Theta \qquad \text{Eq. 1}$$

where Θ is the moment of inertia of the flux surface and $\langle m \rangle$ is the mean mass of thermal ions per electron. In the absence of fast particles and since deuterium and the nuclei of all dominant impurities have an equal number of protons and neutrons we would find $\langle m \rangle \approx$ 2amu. During one slowing down time after the onset of NBI, $\langle m \rangle$ decreases. For the discharge presented in Fig.1 this takes about 300 msec, after which we find $\langle m \rangle \approx$ 1.6amu.

The rotation induced by the beams is parallel to the plasma current, and we define this direction as positive. The frequency of toroidal rotation is taken to be the same for all ion species. According to a neo-classical theory [8] there will be a difference between the rotation speed of carbon and of deuterium. Using this theory we find that the expected difference under conditions relevant for this paper is of the order of the statistical errors of the measurement [9] and can therefore be ignored.

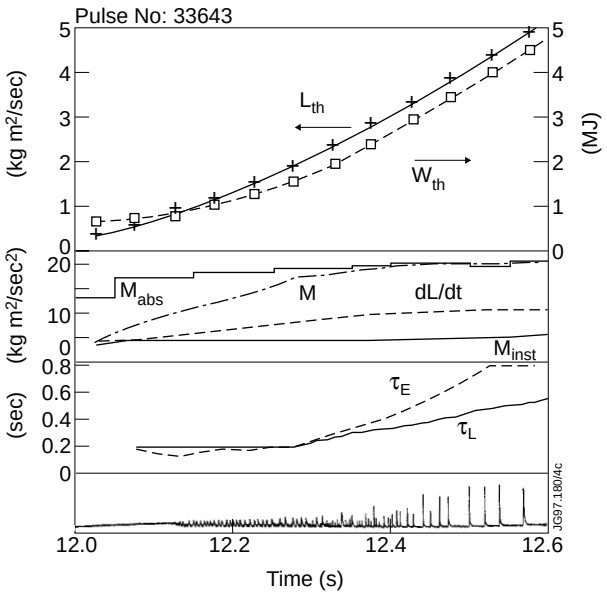

Fig.1: Example for the time evolution during the first 0.6 secs after the onset of NBI. Each time point represents an interval of 50 msec. ***First frame****: The total angular momentum of thermal particles, L_{th} (+), exhibits a more uniform rate of rise than the thermal plasma energy, W_{th} (□).* ***Second frame****: Angular momentum balance showing the time derivative of smoothed toroidal angular momentum, dL/dt. Also shown are the results of the calculations presented in section 3 for the total absorbed NBI torque, M_{abs}, the total torque exerted on the bulk plasma by the fast ions, M,. and the instantaneous torque, M_{inst}, which is roughly constant in time.* ***Third frame:*** *Result for toroidal angular momentum confinement time of thermal particles, τ_L, (see section 4) and thermal energy confinement time, τ_E, which are approximately equal during the L-Mode and during the grassy-ELM phase, but start to differ as the ELM frequency decreases.* ***Fourth frame:*** *Time evolution of Dα signal.*

Time derivatives of angular momentum and thermal energy are calculated by fitting a second order polynomial through five (-2,+2) data points [10]. At the beginning of the time interval the polynomial is fitted through (-1,+3) data points.

2.2. Observations at the onset of NBI

When the beams are turned on the toroidal angular momentum of thermal ions is observed to rise at a rate that, for the example given in this paper, corresponds to a torque of about 4 Nm initially, rising to 10 Nm after 400 msec, Fig. 1. The thermal energy, in contrast, exhibits a change of the rate of rise which corresponds to a power of about 1 MW initially rising to 10 MW after 400 msecs. The behaviour of the energy is consistent with the slowing down of fast ions [2] and an energy confinement time of 0.2-0.3 secs during the first 400 msec. In Figs. 2a and 2b we show that the observed initial rise of angular momentum is due to a rapid change of the rotation frequency between one third and two thirds of the minor radius. For the rotation speed in the plasma centre there is little change initially, followed by a more rapid rise after 200 msec, Fig.2c.

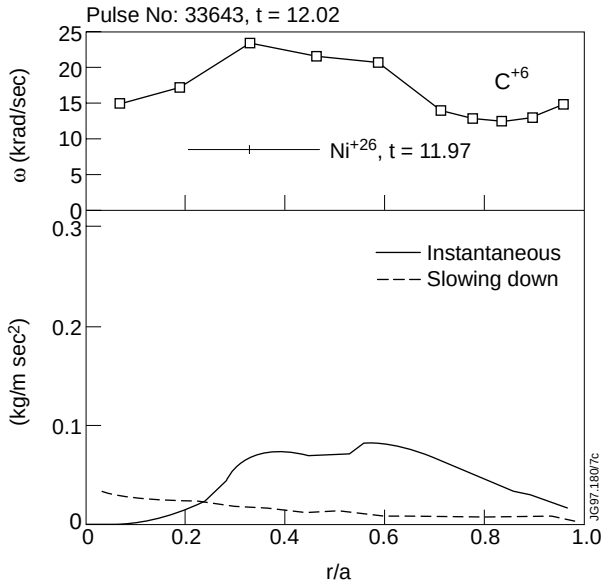

Fig.2a) ***Top:*** *Toroidal angular frequency of C^{+6} averaged during the first 50 msec after the start of NBI. Also shown is the line-of-sight averaged rotation frequency of Ni^{+26} before the NBI phase. The statistical error for each data point is 1-2 krad/sec, the error of the absolute calibration is 5 krad/sec. The radial position and width of the Ni^{+26} emission shell are indicated.* ***Bottom:*** *Calculated torque density profiles (see section 3) for the same time interval showing instantaneous torque and slowing down torque. The radial shape of the total torque density and the observed rotation frequency both have an off-axis maximum during this phase. Note that the torque density here and in Figs 2b) and 2c) are shown on the same scale.*

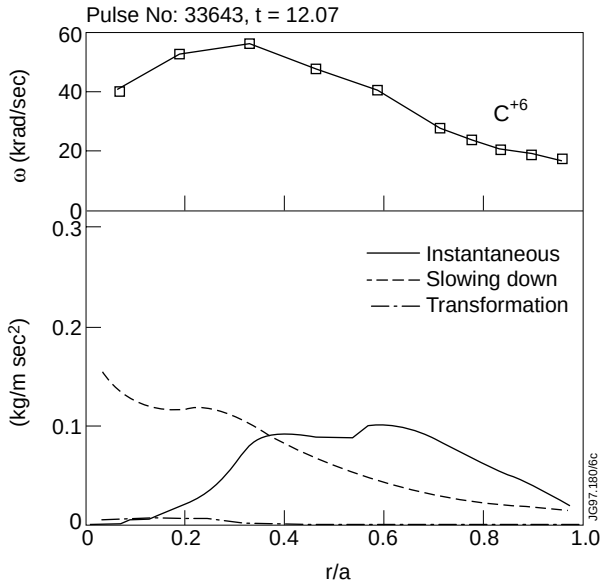

Fig.2b) Like 2a), but averaged between 50 msec and 100 msec after the start of NBI. At this time the slowing down torque starts to become comparable to the instantaneous torque, and the transformation torque begins to appear. The off-axis maximum begins to disappear.

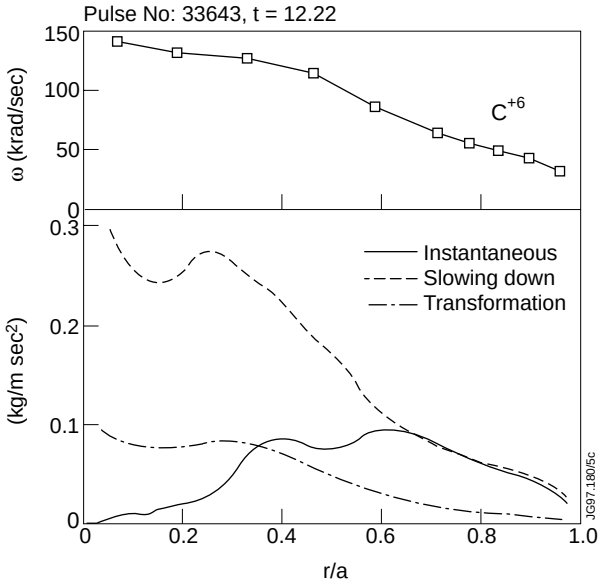

Fig.2c) Like 2b), but averaged between 200 msec and 250 msec after the start of NBI. At this time the slowing down torque dominates, and the transformation torque becomes comparable to the instantaneous torque. The off-axis maximum of the rotation frequency has disappeared, since the latter two contributions peak on axis.

Furthermore, we find that the initial central and edge value of 10 krad/sec is, within the errors of the calibration, the same as measured before the onset of NBI from the spectra of helium-like nickel [11,10] at approximately one third of the minor radius. This indicates that the off-axis maximum is not a feature of the ohmic plasma before the onset of NBI.

These observations clearly demonstrate that toroidal angular momentum is transferred to the bulk faster than can be explained by momentum transfer by collisional slowing down, and that other mechanisms are required to explain the observed behaviour. Particularly striking is the off-axis peak of toroidal rotation since the beam deposition peaks in the central region at all times.

3. MODEL FOR MOMENTUM TRANSFER

What we can see experimentally are only changes in the toroidal angular momentum of thermal ions. The momentum transfer from the beams to these thermal ions occurs in two steps. First, the toroidal angular momentum of the plasma as a whole, which includes thermal as well as fast ions, is enhanced by ionisation of neutrals. We call this the absorption of toroidal angular momentum. Then the fast ions transfer their toroidal angular momentum to the bulk.

3.1. Beam geometry and beam deposition

The beam trajectory intersects each flux surface two times for normal beams and four times for tangential beams, Fig.3. The beam density perpendicular to the beam path has a bi-Gaussian density profile of ellipsoidal shape. In our beam deposition code the beam is cut into slices along

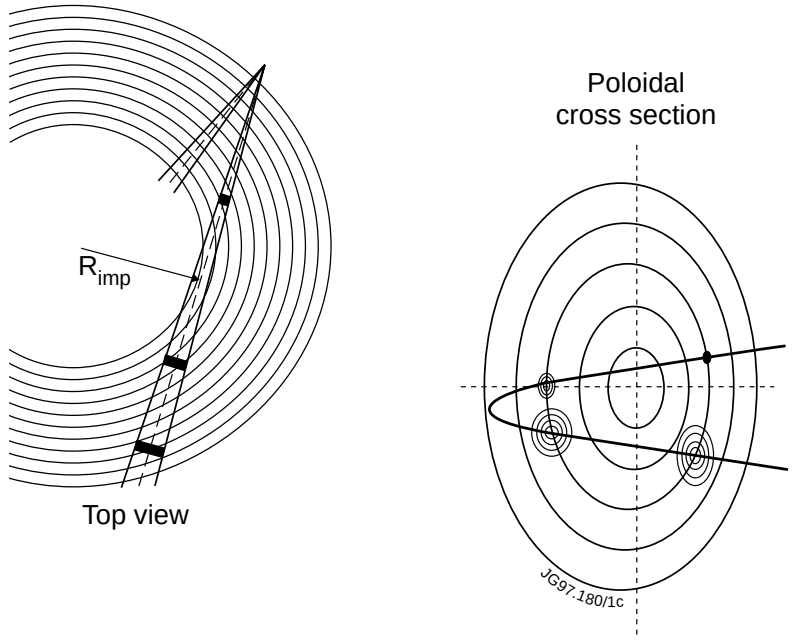

Fig.3: Sketch (not to scale) of typical trajectories for so-called normal and tangential beams. On each flux surface a tangential beam appears four times, two times inboard and outboard. A normal beam appears only twice. The projected beam cross-section changes its shape, from elongated ellipses outboard to more circular ellipses inboard.

the beam path which are then mapped onto flux surfaces to give the number of particles born on each flux surface per time interval.

Beam particles can be absorbed inboard, in which case they become passing ions, or outboard in which case they can become either passing or trapped ions depending on the inverse aspect ratio of the flux surface, $\varepsilon = \frac{r}{R}$. For the axis of normal neutral beams, the particles are passing, i.e. $\xi = \frac{R_{\text{imp}}}{R} > \xi_t = \sqrt{\frac{2\varepsilon}{1+\varepsilon}}$ for $\rho < 0.29$, while for the tangential neutral beam bank they are passing for $\rho < 0.47$. Due to the beam divergence these limits are smeared out.

The absorbed toroidal angular momentum per beam particle is independent of the major radius of the place of birth of the ion, R_I for inboard or R_O for outboard, and given only by the beam line geometry

$$L_{I,O} = m\xi \mathrm{v}_{\text{Beam}} R_{I,O} = m \mathrm{v}_{\text{Beam}} R_{\text{imp}} \qquad \text{Eq. 2}$$

where m is the mass, ξ is the pitch angle, and v_{Beam} is the velocity of the beam. R_{imp} is the impact parameter of the beam path with the torus axis, Fig. 3.

3.2. Momentum transfer from beam ions to the bulk plasma

In the rotating plasma frame ions are born with shifted velocity and modified pitch angle

$$v' = \sqrt{v_{Beam}^2 - 2 v_{Beam} \omega R_{imp} + \omega^2 R_{I,O}^2} \qquad \text{Eq. 3}$$

$$\xi' = \frac{v_{Beam}}{v'} \frac{R_{imp}}{R} - \frac{\omega R_{I,O}}{v'} \qquad \text{Eq. 4}$$

The initial toroidal angular momentum in this frame depends on the point of birth

$$L'_{I,O} = m \xi' v' R_{I,O} = m v_{Beam} R_{imp} - m \omega R_{I,O}^2$$

The ions have three constants of motion between collisions: kinetic energy, magnetic moment and the toroidal component of the canonical angular momentum. The toroidal angular momentum itself is not a constant of motion. For the plasma as a whole, however, both energy and toroidal angular momentum are conserved. Therefore, if one particle loses toroidal angular momentum, other particles have to gain and equivalent amount.

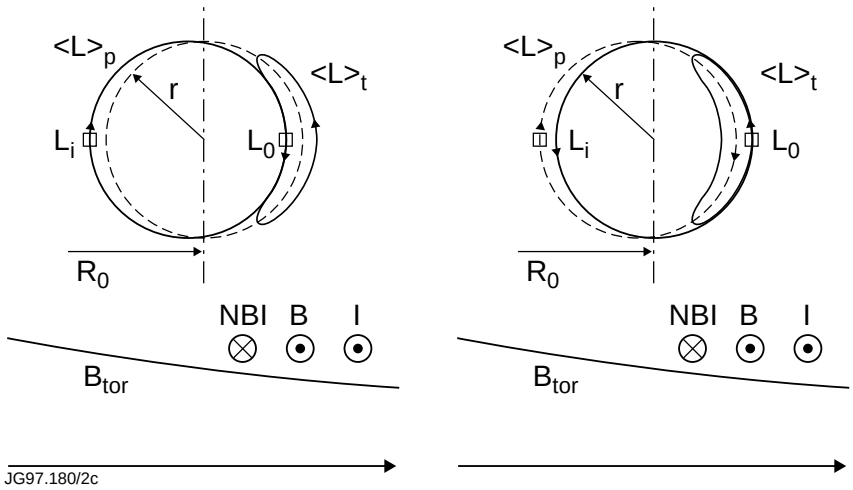

Fig.4: Sketch of drift surfaces for passing particles, absorbed inboard or outboard, and trapped particles. The toroidal angular momentum averaged over the passing orbit, $\langle L \rangle_p$, is larger than L_I at the point of absorption inboard, and smaller than L_O at the point of absorption outboard. The toroidal angular momentum averaged over the trapped orbit, $\langle L \rangle_t$, is much smaller than L_O. This applies to counter-injection (left) and co-injection (right). In JET co-injection is realised.

For ions injected parallel with the plasma current the drift surfaces are shown in Fig.4. The trajectories in the toroidal field result in a variation of the toroidal angular momentum and in addition, because the average minor radius over one drift surface is different from the minor radius at birth, there is a radial current which acts in the poloidal magnetic field to accelerate or brake the fast ions toroidally. Both mechanisms have the same effect, i.e. the toroidal angular momentum averaged over the drift surface is larger than the initial toroidal angular momentum for particles absorbed on the inboard side, and smaller for passing particles absorbed on the

outboard side. For trapped particles it is much smaller, and is given by the rate of precession of the banana orbit around the torus in the presence of the radial electric field that is set up by the rotating plasma.

$$\vec{E} = \frac{\nabla p}{Zen} - \vec{v} \times \vec{B} \qquad \text{Eq. 5}$$

Here we neglect the first term.

In order to maintain quasi-neutrality, there has to be a radial displacement current which in turn exerts a toroidal torque on the bulk [3]. Thus the toroidal angular momentum of the system is conserved, and we find that the difference between the toroidal angular momentum at birth and the first orbit average is transferred instantaneously

$$L_{\text{inst}} = \begin{cases} L'_{I,O} - \langle L \rangle_p & ; \xi > \sqrt{\dfrac{2\varepsilon}{1+\varepsilon}} \\ L'_{I,O} - \langle L \rangle_t \approx L'_{I,O} & ; \xi < \sqrt{\dfrac{2\varepsilon}{1+\varepsilon}} \end{cases} \qquad \text{Eq. 6}$$

The remaining toroidal angular momentum will be transferred by collisions with bulk ions and electrons [2]. During this slowing down process there is no more movement of the fast ions along the minor radius direction. Only the deviation of the particles from the flux surface is reduced. In the laboratory frame there is a third transfer mechanism, which is even slower. The toroidal angular momentum of the bulk is enhanced when the ion has slowed down and is counted as thermal. This transformation torque is given by

$$L_{\text{Trans}} = m_b \omega \Theta \approx m_b \omega R^2 \qquad \text{Eq. 7}$$

It can be seen that the sum of the three contributions is equal to the absorbed toroidal angular momentum in the laboratory frame of reference.

The result of the calculations are illustrated in Fig.1 and Figs 2a-c. The instantaneous torque is roughly constant in time, and changes only due to changes in beam attenuation. It is entirely responsible for the initial rate of rise of the total toroidal angular momentum. The off-axis peak in the rotation frequency during the first 50-100 msec corresponds to the off-axis peak in the calculated torque density. After 200 msec, when the slowing down torque and the transformation torque dominate, the rotation frequency has its maximum on axis.

4. APPLICATION

The thermal energy confinement time τ_E and angular momentum confinement time τ_L are defined as

$$\tau_E = \frac{W_{th}}{P - \dot{W}_{th} - \dot{W}_{\mathrm{rot}}} \qquad \text{Eq. 8}$$

$$\tau_L = \frac{L}{M - \dot{L}} \qquad \text{Eq. 9}$$

This definition includes the effects of viscous heating in the power balance. We have applied our model for the power [2] and torque to the analysis of these confinement times for a variety of JET discharges: L-mode, steady-state ELMy H-mode and hot-ion H-mode discharges.Fig. 5 shows data from 55 JET discharges performed during the 94/95 campaign with the Mark-I divertor.

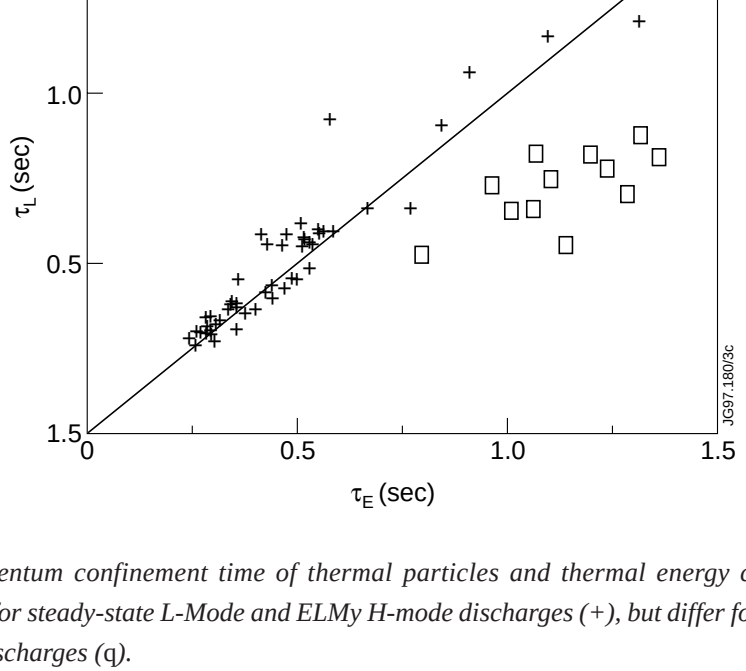

*Fig.5: Angular momentum confinement time of thermal particles and thermal energy confinement time are approximately equal for steady-state L-Mode and ELMy H-mode discharges (+), but differ for the ELM-free phase of hot-ion H-Mode discharges (*q*).*

The confinement times reflect the rate at which energy and angular momentum are first deposited in the plasma bulk, then transported to the edge, and lost from the edge. It is found on JET and on other tokamaks [1] that the toroidal angular momentum and thermal energy confinement times with co-injected neutral beam heating are approximately equal under steady state conditions defined as $\left|\dot{W}_{\mathrm{th}}\right| < 2\,\mathrm{MJ/sec}$ and $\left|\dot{L}\right| < 2\,\mathrm{kg\,m^3/sec}$. It has also been found on several tokamaks that the bulk transport of angular momentum and energy is correlated [12,13],

and during steady-state where torque and power have similar profiles these results suggest that the loss rate at the edge is also identical, dominated by the ambipolar particle flux, heat conductivity and viscosity across the separatrix. However in the ELM-free phase of the high performance hot-ion H-mode discharges we find that the angular momentum confinement time is about 0.6 times the energy confinement time. The difference builds up in time as the ELM frequency decreases, see Fig.1.

The difference can be explained by the improved confinement conditions during the ELM-free phase. Charged particle losses, heat conductivity and viscosity across the separatrix are reduced, so that losses due to charge exchange collisions with neutrals released from the wall, or due to gas puffing, can play an important role in the balance of energy and toroidal angular momentum. Only the ions are affected by this process. Since ions carry about half the energy, whereas, due to their large mass, they carry almost all the angular momentum we find that the energy confinement time is almost doubled with respect to the angular momentum confinement time.

5. SUMMARY AND CONCLUSIONS

We have demonstrated experimentally that there is a difference between the transfer rates of toroidal angular momentum and energy during neutral beam injection. The additional rise of angular momentum occurs in JET between one third and two thirds of the minor radius, and can be explained by $\vec{j} \times \vec{B}$ transfer due to particles injected into trapped orbits: the radial movement between the point of birth and the first orbit average corresponds to a radial current, which brakes the fast particles toroidally. The bulk accelerates due to the radial displacement current that is induced to maintain quasi-neutrality. The radial location where this process occurs is determined by the beam geometry.

We have developed an analytical model for the torque that takes these first orbit forces into account, and which is quantitatively consistent with the observations. The calculation of a further term in the slowing down calculation arising from the scattering of initially passing particles across the trapping boundary will be the subject of future theoretical work.

We have applied our model for the torque and power to the study of toroidal angular momentum confinement times and thermal energy confinement times under steady-state conditions and in transient, hot-ion H-mode plasmas in JET. We find that the two confinement times are about equal in steady-state conditions, but that the angular momentum confinement time is about a factor two smaller than the energy confinement time in the ELM-free phase of hot-ion H-mode plasmas. This difference can be explained by the improved confinement. Losses due to convective and conductive transport across the separatrix are reduced, and therefore losses due to charge exchange with neutrals, which are always present, become apparent.

ACKNOWLEDGEMENTS

None of the spectroscopic measurements would be possible without the skilful technical support by B Viaccoz. We would like to thank D O'Brien and D Muir for producing equilibrium and ECE data with time resolution matched to our requirements.

REFERENCES

[1] A Kallenbach, H-M Mayer, G Fussmann, V Mertens, U Stroth, O Vollmer, and the ASDEX Team, *Plasma Physics and Controlled Fusion*, **33**, 595 (1991)

[2] W G F Core and K-D Zastrow, JET-R(96)01

[3] F L Hinton and J A Robertson, *Phys. Fluids* **27**, 1243 (1984)

[4] R J Goldston, Proc. of Course and Workshop on Basic Physical Processes of Toroidal Fusion Plasmas, Varenna, Italy, 1985, Vol 1, p. 165

[5] N Asakura, R J Fonck, K P Jaehnig, S M Kaye, B LeBlanc, and M Okayabashi, *Nuclear Fusion,* **33**, 1165 (1993)

[6] M Danielsson, M G von Hellermann, E Källne, W Mandl, H W Morsi, H P Summers and K-D Zastrow, *Rev. Sci Instrum* **63**, 2241 (1992)

[7] M G von Hellermann, P Breger, J Frieling, R König, W Mandl, A Maas and H P Summers, *Plasma Physics and Controlled Fusion* **37**, 71 (1995)

[8] D P O'Brien et al, *Nuclear Fusion* **32** (1992) 1351

[9] Y B Kim, P H Diamond, and R J Groebner, *Phys. Fluids* **B3**, 2050 (1991)

[10] L-G Eriksson, E Righi, and K-D Zastrow, *Plasma Physics and Controlled Fusion* **39**, 27 (1997)

[11] W H Press, S A Teukolsky, W T Vetterling and B P Flannery, *Numerical Recipes*, Cambridge University Press 1992, 2nd Edition, p. 644 ff.

[12] R Bartiromo, F Bombarda, R Giannella, S Mantovani, L Panaccione, and G Pizzicaroli, *Rev. Sci. Instr,* **60,** 237 (1989)

[13] S D Scott et al, *Phys. Fluids* **B2**, 1300 (1990)

[14] H P L deEsch et al, Proc. of 17th EPS Conf. Contr. Fusion, Amsterdam 1990, Part I, p. 89